9-2017

Effects of salinity and wet–dry treatments on C and N dynamics in coastal-forested wetland soils: Implications of sea level rise

Xijun Liu
Anhui Agricultural University

Alexander Ruecker
Clemson University

Bo Song
Clemson University

William H. Conner
Clemson University

Alex T. Chow
Clemson University, achow@clemson.edu

Effects of Salinity and Wet–dry Treatments on C and N Dynamics in Coastal-Forested Wetland Soils: Implications of Sea Level Rise

XIJUN LIU[a,b], ALEXANDER RUECKER[b], BO SONG[b], JING XING[c], WILLIAM H. CONNER[b], ALEX T. CHOW[b,d]*

[a] Key Lab of Silviculture, School of Forestry and Landscape Architecture, Anhui Agricultural University, Hefei, Anhui Province 230036, China

[b] Baruch Institute of Coastal Ecology and Forest Science, Clemson University, South Carolina 29442, United States

[c] Department of Computer, Anhui Vocational College of Grain Engineering, Hefei, Anhui Province, 230011, China

[d] Department of Environmental Engineering and Earth Sciences, Clemson University, South Carolina 29631, United States

*Corresponding Author: Tel.: + 8435461013-232

Email address: achow@clemson.edu.

Abstract

Forested wetlands dominated by baldcypress (*Taxodium distichum)* and water tupelo *(Nyssa aquatica*) are commonly found in coastal regions of the southeastern United States. Global climate change and in particular sea level rise will alter the frequency and magnitude of wet/dry periods and salinity levels in these ecosystems. Soil microcosm experiments were set up to identify the effects of water level variations (0.4-3.0 g-water g-soil^{-1}) and salinity changes (0, 1 and 5 ppt of NaCl) on greenhouse gas emissions (CH_4, CO_2 and N_2O) and dissolved organic carbon (DOC) characteristics from forested wetland soils. Our results indicate that, the effect of water level was much greater than salt intrusion on C and N cycling. Wet-dry treatments significantly decreased DOC production and total CH_4-C loss, aromatic and humic-like substance compounds in DOC were increased in both flooding and wet–dry treatments after 60-d incubation. The molecular weight (MW) of DOC after flooding treatments was higher than that in wet-dry treatments. A first order kinetic model showed there was a positive linear correlation (r^2=0.73) between CO_2 emission rate and DOC concentration which indicated that CO_2 was mainly generated from DOC. An exponential kinetic model was applied to describe the correlation between CH_4 emission rate and DOC concentration (r^2=0.41). This study demonstrates that an increase in salinity, and in particular variations in wet-dry cycles, will lead to changes in the formation of climate-relevant greenhouse gases, such as CH_4, CO_2, and N_2O.

Keywords: Dissolved Organic Carbon; Greenhouse Gases; SUVA; Tidal Wetlands

Introduction

Climate change, and in particular sea level rise, is impacting coastal forest and wetland ecosystems. The mean rate of sea level rise in the past 10 years has been exceeding the mean rate of global sea level rise of 0.19 m, reported from 1901 to 2010 (IPCC, 2014). Sea level rise leads to an increase in salt water intrusions (Donato et al., 2011; Breithaupt et al., 2012; Chow et al., 2013) and soil inundation and moisture, which implies greater risks and frequency of flooding (Zhu and Cheng, 2013; Woodruff et al., 2013) and increased soil drying–rewetting cycles (Morillas et al., 2015). Coastal forested wetlands will be among the environments most likely impacted by a combination of alterations in soil biogeochemistry experiencing saltwater intrusions in the next 50-100 years (Schofield, 2003; Allen et al., 1996; Renaud et al., 2015; Donato et al., 2011; Breithaupt et al., 2012; Chow et al., 2013) and hydrology due to changed wet-dry dynamics. Of particular interest are alterations in SOM (soil organic matter) levels and DOC (dissolved organic carbon) structure, which will affect carbon sequestration, soil microbial activity, and consequently biogeochemical element cycling and soil to air gas exchange (Moyano et al., 2013; Chow at el. 2003, 2005; Lal, 2004; Moseman-Valtierra et al., 2011).

Previous studies have demonstrated that decomposition rate of DOC (Fierer and Schimel, 2002) and the quantity, as well as, the chemical characteristics of DOC are affected by water level fluctuations and wet–dry cycles (Lundquist et al., 1999; Kalbitz et al., 2000; Chow et al., 2003). Positive correlations between C mineralization rate and DOC concentration were found in coastal wetlands (Cook and Allan, 1992; Chow et al., 2006). The impact on greenhouse gas formation however, remains poorly understood. While Shi and Marschner (2014) reported an increase in GHG formation as a consequence of varying water levels, Morillas et al. (2015) reported a decline in GHG formation based on a lower microbial biomass and microbial activity.

In addition to fluctuations in water levels, the intrusions of sea water into coastal freshwater environments is of particular interest as higher salt concentrations will contribute to changes in biogeochemical turnover of C and N (Chow et al., 2013; Lewis et al., 2014). Recently the consequences of freshwater wetland salinization have been summarized in a review by Herbert and colleagues (Herbert et al., 2015). Therefore, we will only mention the most important impacts on N and C dynamics and refer the reader to the work by Herbert et al. (2015) for an in-depth discussion on the impacts of wetland salinization. The combination of an enhanced N mineralization and dissimilatory nitrate-reduction coupled to

ammonium, a reduced nitrification-denitrification, and an increase in NH_4^+ are the direct consequences of saltwater intrusions on N dynamics in wetlands (Ardón et al., 2013). Interestingly it has been demonstrated that an increase in salinity can also have a stimulating effect on nitrification in saline soils and that an inhibition only occurred when electric conductivity (EC) exceeded 16,000 µS cm^{-1} (Ardón et al., 2013).The main consequence of increasing salinities on carbon dynamics is a decrease in plant productivity, and hence carbon inputs to the soil. Additionally, it will cause a decrease in microbial activity and consequently slower DOC decomposition rates (Setia et al., 2013)**.** In particular, salinization affects solubility and mobility of DOC and potentially the formation of CH_4 (Ardón et al., 2016; Mulholland, 1981; Sholkovitz, 1976). Therefore, an increase in salinity as it occurs in coastal saline wetlands may lead to lower CH_4 emission rates compared to freshwater wetlands (Baldwin et al., 2006; Marton et al., 2012).

As the changes in C turnover occur, it can be expected that the turnover of N, and in particular the formation of the greenhouse gas nitrous oxide (N_2O) will be affected, too. Previously, it has been demonstrated that emission of N_2O is the primary pathway of N loss from wetland soils into the atmosphere, and that variations in water levels and conductivity affect N_2O emissions from an alkaline soil (Silva et al., 2008; Kraus and Whitbeck, 2012). The impacts of different salinities in combination with varying water levels on N_2O formation has, to the best of our knowledge, not yet been investigated. The above mentioned aspects illustrate the necessity of a thorough quantification of greenhouse gas emissions under varying water levels and salinities to gain a better understanding of potential alterations in atmospheric levels of these climate-relevant gases. In particular, the contribution of different C and N fractions (DOC, soil organic carbon (SOC), total nitrogen (TN), and soil nitrogen (SN) as precursors for greenhouse gas formation is also of interest. Additionally, the identification of DOM optical properties is essential as it serves as a C source for microorganisms in the soils and is crucial for biogeochemical turnover of C and N.

The flow of C and N through soil is inherently complex. Many thousands of different chemical transformations and physical processes occur simultaneously within the soil matrix. Instead of tracking individual reactions and processes, kinetic models based on empirical and experimental data can predict the flows of C and N even if the reaction mechanisms are not known (Glanville et al., 2016). These approaches have been used to described different nutrient cycling in wetland soils (Chen and Rudolf, 2016; Chow et al. 2006; Chow et al., 2004). Results of the kinetic model could also provide insights about the

biogeochemical processes within soil matrix. For example, Chow et al. (2006) used a 1st order kinetic model to demonstrate that CO_2 was mainly produced from DOC in soil pore water under oxidized condition, whereas CO_2 was produced from SOC under reduced conditions. However, the relationships of CH_4 and N_2O emissions on DOC and DTN, as well as impacts of salinity have not examined before.

Therefore, the overall goals of this study were (I) to quantify greenhouse gas emissions (CO_2, N_2O, and CH_4) under varying salinities, and water levels, (II) to demonstrate the effects of varying salinities and water levels on DOM optical properties and (III) to develop a kinetic model to elucidate the contribution of different C fractions to CO_2 and CH_4 formations in our microcosm experiments.

2. Materials and experimental methods

2.1. Field site and sampling procedure

The study was conducted with soil samples from a healthy forested wetland on Hobcaw Barony (33º21′N, 79º12′W), near Georgetown, South Carolina, which is currently not affected by saltwater intrusions. The highly productive (average annual litterfall input of 620 g m^{-2} yr^{-1}; Conner, unpublished), seasonally flooded 24-ha (2.4×10^5 m^2) wetland is dominated by baldcypress (*Taxodium distichum* (L.) Rich.), water tupelo (*Nyssa aquatica* L.), and swamp tupelo (*Nyssa biflora* Walt.) trees. The surrounding forest community included longleaf pine (*Pinus palustris* Mill.) and turkey oak (*Quercus laevis* Walt.) (Busbee et al., 2003). The predominant soil type in this wetland has been characterized as a fine-loamy, siliceous, thermic, and Yypic Ultisol (USDA Soil Taxanomy) (Stuckey, 1982). Detailed characterizations of this site, including tree composition, stem density, aboveground productivity, litterfall, nutrient dynamics, and hydrology have been published previously (Busbee et al., 2003; Chow et al., 2013). Surface soil samples were collected from 0–10 cm after removal of litter from the surface during the wetland's dry period in the summer. The soils were transported to the laboratory, air-dried at room temperature (22 ± 1°C) until constant weight, sieved to a particle size < 2 mm for homogenization, and stored at room temperature until further analysis and start of the soil incubation experiments. This homogenization might have impacted the microbial activity or microbial community. Therefore, results from the laboratory microcosm incubations presented here are not directly transferable to results that can be expected from the field. Relevant soil characteristics are summarized in Table 1.

142 **2.2. Setup of microcosm experiments and sampling procedure**

143 Microcosm experiments for the quantification of greenhouse gas formation in varying approaches were set
144 up using one-liter mason jars. Each jar contained 50 g of dried ground surface soil and 150 g of deionized
145 water or solutions of 1 ppt and 5 ppt NaCl, to simulate freshwater and two levels of oligohaline-degraded
146 wetlands with the dieback of some trees in the canopy layer (Cormier et al., 2013). Hereafter the 3 setups
147 are labelled as 0, 1, and 5 ppt. Soils were incubated either under constant flooding conditions or wet-dry
148 cycles of 12-d for a total of 60 days at room temperature. Besides the 3 different salinities, we applied two
149 different water levels (permanent flooding, and wet-dry cycles). A total of 120 jars were used (18 jars x 6
150 treatments + 12 blank controls). All jars were incubated at room temperature in the dark. In the flooding
151 experiment, each jar was covered by a lid with a 2-mm opening to allow for gas exchange. The θ_g in each
152 jar was monitored regularly by gravimetric measurement. Water content was readjusted with deionized
153 water when a 5% or more change in θ_g occurred. In the wet–dry cycle incubation experiment, surface soils
154 were initially flooded with a θ_g of 3.0 g-water g-soil^{-1}. All jars were incubated at room temperature without
155 lids so that soil samples were allowed to dry naturally through evaporation. When the soils reached the
156 desired θ_g values, soils were re-flooded to their initial θ_g with deionized water for continued incubation.

157 For pH, electrical conductivity (EC), DOC, dissolved nitrogen (DN), UV-VIS, and
158 spectrofluorometry, three replicates of each incubation condition were terminated at 12, 24, 36, 48, and 60-
159 d. To obtain water extracts, deionized water was added to the original water level (150 g of water to 50 g
160 soil) and shaken rigorously for 5 minutes and then filtered through a 0.45μm membrane filter (Millipore
161 Express) prior to analysis. All samples were kept at 4 °C and analyses were completed within a week. In
162 addition to the DOC extraction, three replicates of each treatment were used to quantify CO_2, CH_4, and
163 N_2O emissions during the 60-d incubation. Eighteen jars for gas measurement were sealed with a gastight
164 lid equipped with a removable rubber septum. The jars were capped every 3 days and gas samples were
165 collected after 24 hours. A septum was used to seal the opening for 24 h before sampling and analysis.
166 Twenty-four ml of gas was withdrawn from the sealed jar for quantification of CO_2, CH_4, and N_2O,
167 expressed as emissions in μg g-soil^{-1} d^{-1}. In addition, three empty jars were used to determine CO_2, CH_4,
168 and N_2O background levels. CO_2, CH_4, and N_2O production from the soils was determined by subtracting
169 the CO_2, CH_4, and N_2O concentrations of the empty jars.

170

171 **2.3. Analysis**

172 Concentrations of C and N in the original soils (0 day) and after 60-d incubation (oven dried at 70 °C for
173 48 h) were quantified using a Thermo Flash EA 2000 element analyzer. CO_2, CH_4, and N_2O were analyzed
174 by a Shimadu Greenhouse Gas analyzer (GC 2014). All filtered solution samples were analyzed for pH,
175 EC, DOC, and DN. The pH and EC of filtered solution samples were determined using an Accumet XL60
176 dual channel pH/ion/conductivity meter. EC was corrected to EC at 25 °C (EC_{25}) using the temperature
177 correction equation: $EC_{25} = EC_t / [1 + 0.021 (t-25)]$ (Hayashi, 2004). The DOC and DN were measured
178 using a Shimadzu TOC/TN analyzer (SM 5310B).

179 DOM optical properties were further characterized by UV-VIS spectrophotometry (Shimadzu UV-
180 1800) and spectrofluorometry (Shimadzu Spectrofluorometer RF5301). All DOC samples also were
181 analyzed for Specific ultraviolet absorbance (SUVA), and one of the 3 replicates was used for
182 spectrofluorometry. Specific ultraviolet absorbance, spectral slope ratio (S_R), and E_2/E_3 ratio were
183 determined as described previously (Chow et al., 2008; Helms et al., 2008; Wang et al., 2015). Based on
184 SUVA and E_2/E_3 ratio, selected samples were analyzed using fluorescence emission-excitation matrix
185 (EEM) (Zhou et al., 2013). Several spectrofluoroscopic indices including the fluorescence index (FI), the
186 freshness index (β/α), and humification index (HIX) were calculated as shown previously (Fellman et al.,
187 2010; Wang et al., 2015; Cory and McKnight, 2005).

188

189 **2.4. Calculation of gas fluxes and statistical analysis**

190 Fluxes of CO_2, CH_4, and N_2O were calculated on the basis of daily data using the ideal gas law. As CO_2,
191 CH_4, and N_2O concentrations were determined every four days, their mineralization rates during sampling
192 intervals were assumed equal to the average of the two mineralization rates from the two sampling events
193 when calculating the cumulative production (Chow et al., 2006). Greenhouse gas fluxes and concentrations
194 of DOC and DN were used to examine the relationship among CO_2–C, CH_4-C and DOC, N_2O-N, and DN.
195 The least squares method was used to construct the best fit between formation of CH_4, and CO_2 and DOC
196 concentration, as well as between N_2O formation, and DN concentration. The slope of each linear
197 regression line was equal to the reaction rate constant for the specific incubation condition. One-way
198 ANOVA (SPSS, 20.0) was used to detect statistically significant differences in the effects of salinity and
199 wet-dry treatments on C and N cycles, respectively.

200

201 **2.5 Development of kinetic model**

202 The above mentioned reaction rates were used to develop a first-order or an exponential kinetic model
203 demonstrating the importance of different carbon fractions (SOM and DOM) in the formation of the
204 greenhouse gases (CO_2, and CH_4) under flooding conditions. Interestingly, our first order or exponential
205 kinetic model was suitable to detect differences in the precursors of CO_2 or CH_4 in the present study. This
206 demonstrates the importance of a thorough DOM characterization and how changes in the salinity can affect
207 C turnover. Unfortunately, we were not able to expand our model to the wet-dry treatment. There are
208 possible two reasons accounting for the limitation using the model in wet-dry treatment. First, the variations
209 in water content most likely affects DOC availability and GHG transport processes in soil. The kinetic
210 model here focuses on the chemical reactions and it does not consider other transportation processes. During
211 the wet-dry processes, water evaporation and other gas transport, which were not accounted in the proposed
212 reaction kinetic model, could be factors affecting DOC concentration and GHG emission. Besides,
213 microbes might be stressed and microbial communities might be altered during the wet-dry processes. The
214 model could not predict the lag phases of GHG or DOC productions.

215

216 One of the reasons for that is, that variations in water content most likely affect DOC availability and its
217 transport processes in soil which cannot be described by the proposed reaction kinetic model. In the kinetic
218 model, daily CO_2-C emission rates (i.e., d[CO_2-C]/dt) were equal to the sum of k_{SOC} [SOC] and k_{DOC} [DOC],
219 where the constants k_{SOC} and k_{DOC} are the reaction rates of SOC and DOC in forming CO_2. The first-order
220 kinetics we used to describe the reaction among d[CO_2-C]/dt, and SOC, DOC was:

221 $$\mathrm{d}\,[CO_2 - C]/dt = k_{SOC}[SOC] + k_{DOC}[DOC]$$

222 In the exponential model, daily CH_4-C emission rate (i.e., d[CH_4-C]/dt) was equal to K_{SOC}exp
223 (K_{DOC}[DOC]), where K_{SOC} is the reaction rate constant or C mineralization rate from SOC to CH_4, and K_{DOC}
224 is solubility or production of DOC from SOC. The correlation equation we used to describe the reaction
225 among d[CH_4-C]/dt and DOC was:

226 $$\mathrm{d}\,[CH_4 - C]/dt = K_{SOC}\, e^{K_{DOC}[DOC]}$$

227 **3. Results**

228 **3.1 Kinetic models for C and N cycles**

229 We observed that total CO_2-C (12.1-12.4 mg-C g-soil^{-1}) and CH_4-C losses (2.6 - 2.9 mg-C g-soil^{-1})
230 after 60-d incubation exceeded initial DOC concentrations (1.0 – 1.2 mg-C g-soil^{-1}) for all treatments
231 suggesting both SOC and DOC could be substrates for CO_2 and CH_4 production (Boyer and Groffman,

1996). However, SOC was considered a relatively large C pool and the change in SOC content within the 60-d incubation should be minimal in comparison to the C changes in gas and water phases. In order to delineate the relationships of the dynamic variables, CO_2-C or CH_4-C was plotted against DOC concentration, as shown in Figure 1a and 1b, respectively. A linear correlation with ($R^2 = 0.73$) between CO_2-C and DOC was observed (Fig. 1a), whereas an exponential correlation ($R^2 = 0.41$) between CH_4-C and DOC was obtained (Fig. 1-b). DOC concentration is the same between CO_2 and CH_4 during the incubation, but there is no CH_4 emitted at the beginning of incubation, so we deleted the high DOC with no CH_4 emission in figure 1-b. We applied a kinetic model to demonstrate the contribution of different carbon fractions and concentrations on formation rates of CO_2 (Chow et al., 2006). Wet-dry treatments are not modeled by this approach because the variation in water content could change DOC availability as well as its transport processes, which cannot be simply described by the reaction kinetic model. In the kinetic model, total available organic carbon (TAOC) is the sum of degradable SOC and DOC, which are available and accessible to microbes during the 60-d incubation. TAOC was not necessarily equal to total organic C in soils because not all of the C would be involved in the reactions occurring during the 60-d period. In addition, DOC could be produced at an independent reaction rate constant k_{SD} by microbes utilizing SOC as C source. The reaction rate constant k_{SD} is not equal to k_{SOC} because the mechanism producing CO_2 is probably different from that producing DOC (Moore and Dalva, 2001; Chow et al., 2006).

The CO_2-C emission rate was linearly proportional to DOC concentration; therefore, we applied the first order kinetic model to describe the relationship. CO_2 emission rate ($d[CO_2\text{-}C]/dt$) is equal to CO_2 production from SOC and DOC, written as k_{SOC} [SOC] and k_{DOC1} [DOC] in equation [1] in Figure s2. After substituting and manipulating the variables as shown in Box in Figure s2, a linear relationship ($y = ax + b$) was obtained as shown in equation [4], where y is the CO_2 mineralization rate ($d[CO_2\text{-}C]/dt$), a is the difference between reaction rate constants (k_{DOC1}-k_{SOC}) alternatively called an apparent reaction rate constant (k_{app}), x is the DOC concentration, and b is the y-intercept and is equal to TAOC concentration with a factor of k_{SOC}. The linear equation [4] in Figure s2 can be used to predict the sources of CO_2 emission. Based on this model, the correlation between CO_2 emission rate and DOC concentrations depends on k_{app}, which is a function of k_{DOC1}, and k_{SOC}. The slope of the linear relationship between CO_2-C emission rate and DOC is positive, indicating that the rate constant of k_{DOC1} representing microbes mineralizing DOC is

greater than the rate constant of k_{SOC} representing mineralizing SOC (Chow et al., 2006). This suggests that microorganisms preferentially utilized DOC to produce CO_2 over SOC.

In contrast to CO_2 emission, the linear equation did not fit well when CH_4 emission rate ($d[CH_4\text{-}C]/dt$) was plotted against DOC concentration. Instead, the CH_4-C emission rate had a relatively close fit (r^2 = 0.41) with an exponential function, as expressed by $d[CH_4\text{-}C]/dt = K_{SOC} \times \exp(K_{DOC}[DOC])$ (Fig. 1b). Here, y is the CH_4-C emission rate and x is DOC concentration. If DOC concentration of the system is zero (i.e. [DOC] = 0), $d[CH_4\text{-}C]/dt$ is equal to K_{SOC} with unit of concentration over time. Therefore, K_{SOC} is the reaction rate constant or C mineralization rate directly from SOC to CH_4 in our system. In addition, K_{DOC} has a unit of an invert of DOC concentration because a value of exponential function should be dimensionless. Therefore, K_{DOC}, with a unit of g-soil / ug-C in our case, is the solubility or equilibrium constant of DOC from SOC. Overall CH_4-C emission rate is a factor of K_{SOC} with an exponential function that depends on the SOC to DOC production. If K_{DOC} is small, the function flattens out, suggesting a slower rate of CH_4-C emission. If K_{DOC} is large, the curve increase rapidly, suggesting a rapid production of CH_4-C. In this study, although we only found a rather weak correlation between DOC and CH_4 (r^2= 0.41), it is conceivable that the activity, and potentially also population size, of Archaea responsible for CH_4 formation increased with increasing DOC concentration, explaining at least to some extent the observed relation between CH_4 and DOC. Nevertheless, it has to be considered that many other factors such as redox conditions play a crucial role for CH_4 formation that are not considered in the equation above and that a good correlation between variables does not imply causality.

The same correlation analyses were done for N_2O formation and DN. The experimental data suggest a negative linear correlation between N_2O and DN (R^2=0.45; data not shown). However, the data set showed two distinct data clouds and thus we can only speculate about the actual contribution of DN to N_2O formation and the factors that are relevant for N_2O emissions from our setups.

3.2 GHG dynamics under salinity and wet-dry treatments

Figure 2 shows formation of CO_2, CH_4, and N_2O from our soil microcosm incubations over 60-d under different salinities and water levels. Results demonstrated that water level significantly altered the patterns of CO_2 emissions but salinity did not (Figs. 2a-c). In the three salinity treatments under permanent flooding (blue line), CO_2 emissions were highest on day 9, with an average of 417.5 (± 15.8), 440.6 (± 8.7), and

464.7 (± 14.6) μg-C g-soil^{-1} d^{-1} at 0 ppt, 1 ppt and 5 ppt of NaCl, respectively, and gradually decreased over time. Considering the highest CO_2 emission rate, an increase in salinity apparently increased the CO_2 emission rate but the differences were not statistically significant ($p > 0.05$). Differences in total CO_2-C losses over 60-d of incubation were 12.2 (± 0.5), 12.4 (± 0.4), and 12.1 (± 0.5) mg-C g-soil^{-1} at 0 ppt, 1 ppt and 5 ppt of NaCl, respectively, and found to be statistically not significant (Table 2). Under the wet–dry cycle treatment, CO_2 flux followed closely with soil water content. The highest CO_2 flux in each cycle occurred 8 days after each re-flooding, and then the CO_2 mineralization rate declined and was lowest when the soils had the lowest θ_g. Moreover, the highest CO_2 flux decreased with wet–dry cycles during the first 8 days of incubation. Total CO_2-C loss during the 60d incubation in wet–dry cycle was 11.7 (± 0.5), 12.8 (± 0.7), and 11.6 (± 0.5) mg-C g-soil^{-1} at 0 ppt, 1 ppt and 5 ppt NaCl treatments, respectively. Generally, total CO_2-C loss under the wet-dry treatment was statistically equal to flooding condition in the 60-d incubations ($p > 0.05$).

CH_4 was not detected until the 12th day of incubation in both wet-dry and flooding treatments. Our results demonstrated that CH_4 formation was mainly influenced by fluctuations in water level, whereas effects of different salinities on CH_4 formation were negligible (Figs. 2d-f). In all salinity and wet-dry treatments, the highest CH_4 fluxes occurred after 21 days of incubation, then decreased to 19%-28% at flooding and 1%-6% at wet-dry contrast to highest fluxes and remained stable until the end of the experiment. Highest CH_4 fluxes from 0, 1, and 5 ppt NaCl were 148.3, 159.7 to 123.0 μg-C g-soil^{-1} d^{-1}, respectively. Wet-dry treatments significantly reduced CH_4 emission rates and total CH_4-C losses from all treatments (Fig. 2).

In contrast, both water level and salinity significantly influenced the emission dynamics of N_2O (Figs. 2g-i). Under flooding conditions, high salinity reduced the peak of N_2O emission rate from 9.0 ng-N gsoil^{-1} d^{-1} (0 ppt NaCl), 5.3 ng-N g-soil^{-1} d^{-1} (1 ppt NaCl) to 0.4 ng-N g-soil^{-1} d^{-1} (5 ppt NaCl), with a total N_2O-N loss of 0.10, 0.08, and 0.02 μg-N g-soil^{-1}, respectively. Under wet–dry cycles, N_2O emissions followed closely with soil water content, especially in the later incubation. Highest N_2O emissions were quantified immediately after re-flooding for each wet-dry treatment and decreased with decreasing soil water content. Interestingly, N_2O emission rate apparently increased at the later cycles of wet–dry incubation. Total N_2O-N losses after 60-d of incubation during wet–dry treatments were 0.22 (± 0.03), 0.17 (± 0.01), and 0.15 (± 0.02) μg-N g-soil^{-1} at 0 ppt, 1 ppt, and 5 ppt NaCl, respectively, which was significantly higher than during

318 flooding ($p<0.05$). Compared to the initial concentrations, TC, TN, and DN in the soil actually decreased
319 for all treatments after 60-d incubation, but changes were not statistically significant. Total C loss (CO_2-C
320 + CH_4-C) after 60-d incubation was 6.2% of original TC, and total N_2O-N loss after 60 days was 0.1% of
321 original TN.
322
323 **3.3 Water quality**
324 The original forested wetland soil pH was slightly acidic with an average of 5.0 ± 0.1 (n = 3), but
325 increased to (6.0 - 7.5) during the 60-d incubation. No significant difference was found among the salinity
326 treatments ($p > 0.05$) although the average pH decreased with salinity. The pH under flooding conditions
327 (6.2 - 7.5) was significantly higher than under wet-dry treatment conditions (5.9 - 6.1) ($p < 0.05$). An
328 increase of pH in soils with increasing salinity is possibly due to the carbonate and a relatively
329 high pH of sea water (pH ~ 8). In our study, we focus on the effect of NaCl. Without the carbonate
330 as buffer reagents, the soil pH could be easily altered. Moreover, a decrease of pH is commonly
331 observed in submerged wetland soils. Organic soil is often acidic during submergence through the
332 slow oxidation of sulfur compounds, producing sulfuric acid, and the production of humic acids
333 (Mitsch and Gosselink, 1993). In fact, we did not observe a decrease in pH in the wet-dry
334 treatment. This suggests that the presence of NaCl is not the main driving force in the observed
335 pH changes.
336 Figure 3 shows the temporal variations of DOC and DN concentrations as well as DOC/DN ratios
337 over 60-d incubation. Original DOC concentrations in all cases were the lowest with 1.2 ± 0.0 mg-C g-
338 soil^{-1} (Figs. 3a-c). After 60-d of incubation DOC concentrations increased significantly under flooding
339 treatments (1.7 ± 0.1 - 2.2 ± 0.3 mg-C g-soil^{-1}) and 5 ppt in the wet-dry treatments (1.6 ± 0.1 mg-C g-soil^{-1}).
340 DOC concentrations were highest after 12 days of incubation and increased 3.4 - 4.5 times under
341 flooding (θ_g = 3.0) and 1.8 - 2.4 times under wet–dry cycles (θ_g = 0.4 - 3.0). The same trend was observed
342 with varying salinities. However, DOC concentrations were significantly higher in the permanent
343 flooding incubation compared to incubation under wet-dry conditions ($p < 0.05$). Although DOC
344 concentrations at 0 ppt and 1ppt NaCl during flooding exceeded DOC concentrations in the 5ppt NaCl

345 treatment, no statistically significant difference in mean DOC concentrations were observed between the
346 salinity treatments ($p > 0.05$).

347 DN concentration had a similar trend over time with varying salinity under both flooding and wet-
348 dry treatments (Figs. 3d-f). DN concentrations increased rapidly from the lowest concentration in original
349 soil (0 day), then fluctuated during the remainder of incubation. DN concentrations under flooding
350 increased 2.9 - 3.6 times after 60-d incubation and more than 2.0 - 3.3 times under wet-dry treatments.

351 The dynamics of DOC/DN ratios were similar to DOC concentration starting at 4.4 - 6.2 and reaching
352 its highest level of 5.7 - 8.7 after 12 days of incubation, then decreasing gradually to 2.5 - 3.0 (Figs. 3g-i).
353 The range of DOC/DN ratios was greater with flooding than that in wet-dry treatments, and with increasing
354 salinity, the peak of DOC/DN ratios was reduced, but ratios after the 60^{th} day were similar.

355

356 **3.4. Optical characterization of DOM**

357 Samples for characterization of DOM optical properties were collected every 12 days and included
358 analyses of SUVA, S_R, E_2/E_3 ratio, and Fluorescence EEM. Similar to the other parameters described above,
359 there were no obvious differences between salinity treatments ($p > 0.05$), but differences were observed
360 between flooding and water level treatments ($p > 0.05$) (Fig. 4). Higher salinity treatments lowered SUVA,
361 but the difference was not statistically significant ($p > 0.05$) during the 60-d incubation (Figs. 4a-c).

362 E_2/E_3 ratios and S_R showed similar temporal trends at different salinities under both permanent
363 flooding and wet-dry treatments, however no statistically significant difference among salinity was found
364 ($p > 0.05$) (Figs. 4d-i). E_2/E_3 ratios under wet-dry treatments were significantly higher than under flooding
365 ($p < 0.05$). In the same incubation period, DOC concentration increased gradually, while E_2/E_3 dropped to
366 its minimum on day 12 in flooding and wet-dry treatments. SUVA and S_R increased and E_2/E_3 ratios
367 decreased over time when comparing values at the beginning of the experiment and after 60 days of
368 permanent flooding. Furthermore, lower SUVA but higher E_2/E_3 ratios of DOC were found at 60-d during
369 wet-dry cycling.

370 Results from 3D fluorescence regional integration and emission-excitation matrix are shown in Fig.
371 5. From fluorescence index (FI), freshness index (β/α), and Fluorescence regional integration, we can
372 conclude that DOM has higher MW in both flooding and wet-dry treatments after 60-d incubation
373 compared to its original properties. Humic-like DOM was the largest component, comprising about 34-

65% of DOM, and protein-like DOM was the second most abundant fraction, comprising 20 to 41% of DOM in all treatments. Although the proportion of various components of DOM fluctuated during the incubation under various salinity and water level conditions, the observed structural changes were statistically not significant ($p > 0.05$) (Fig. 6). Compared to original DOM, fulvic-acid like and humic-acid like DOM are the most dominant fractions after 60 days.

4. Discussion

4.1 Contribution of different C fractions to GHG formation

The linear relation between DOC and CO_2 emissions suggests that CO_2 is mainly formed from DOC and that SOC only contributes to a minor extent to CO_2 emissions from our microcosm experiments. In contrast to that, an exponential function was applied to fit CH_4 formation in our setups. Initially we also applied a linear model to our CH_4 data, however we did not find a correlation between DOC and CH_4 (data not shown). In a next step we used a second order quadratic model which showed a relatively good correlation between DOC and CH_4 (R^2=0.70) but this model does not make sense from a biogeochemical point of view as it is based on an initial decrease in DOC with a simultaneous increase in the emissions of CH_4. Therefore, we developed an exponential model to describe the contribution of DOC to CH_4 formation in our microcosms under permanent flooding conditions. Although the correlation was considerably weaker (R^2=0.41) than observed for the quadratic model, we believe that it better describes the actual relationship between DOC and CH_4.

However, it also demonstrates that the formation of CH_4 in our setups is more complex than the formation of CO_2 and that many other factors besides the availability of DOC play an important role for CH_4 formation. Some factors that might be of importance are redox conditions but also the competition between methanogens and other strictly anaerobic microorganisms, such as sulfate reducers and Fe(III)-reducers might play a role. Nevertheless, we can only speculate about the underlying formation mechanism and the contribution of DOC to CH_4 formation as correlations are only a statistical tool and do not imply causality. The observed differences in the precursor substances of CO_2 and CH_4 are still of great relevance in regard to global climate change. Rising mean temperatures will affect soil C decomposition rates and thus carbon structure which might lead to alterations in the formation rates of the greenhouse gases CO_2 and CH_4

(Davidson and Janssens, 2006). However, these conclusions are based on laboratory soil incubations and in how far these results are transferable to conditions in the environment is currently unknown.

4.2 Carbon –salinity, water level (flooding and wet-dry)

4.2a Carbon – salinity vs water level

Rising sea level has increased the hydroperiod and salinity in low-lying coastal freshwater forested wetlands (Krauss and Whitbeck, 2012). These environmental changes alter the C and N biogeochemical processes in wetland soils in different ways. Our experiments suggest that an increase in salinity under oligohaline conditions (≤ 5 ppt) did not significantly alter C cycling in terms of CO_2/CH_4 emission and DOC production (Figs. 5 a and c). For gas emissions, our results are in line with a previous study showing no effect on CO_2 or CH_4 emission with mean pore water salinity ranging from 0.2 to 4.7 ppt in the same type of forested wetland (Krauss and Whitbeck, 2012). Results suggest the impacts of low levels of saltwater intrusion on CO_2 and CH_4 productions from coastal wetland soils were negligible. However, it has been demonstrated that fluctuations in salinity affect DOC production in coastal wetlands (Olsen et al.,1996; Ardón et al., 2016; Chambers et al., 2014). Olsen et al. (1996) and Ardón et al. (2016) demonstrated that saltwater intrusions could reduce DOC in leachate while Chambers et al. (2014) showed an increase in DOC concentration in soil pore water. Our study did not observe any differences among salinity treatments after 60-d incubation. While CO_2 and CH_4 emissions are mainly controlled by microbial processes, DOC concentrations and exports are the result of a combination of environmental biotic and abiotic factors (Chow et al., 2003). The inconsistencies among studies are probably due to the involvement of several physical (e.g., coagulation and adsorption), chemical (e.g., photochemical and redox processes), and biological (e.g., microbial production and decomposition) processes during DOC production in soil water (Zsolnay, 2003). In this study, we specifically investigated the effects of NaCl and hydroperiod on freshwater wetland soils under low salinity levels (≤ 5 ppt) for a period of 60 days. An increase in DOC during the incubation was mainly due to the effects of water level (see section 4.2b). Results demonstrated that the effect of salinity on C cycling in oligohaline environments in a short period of time is negligible. Water level or the hydroperiod is the driving force on C cycling under oligohaline conditions. However, it has to be considered that results from a simplified laboratory incubation cannot directly be transferred to conditions in the field which are much more complex. In particular, the choice of salt can be of relevance.

Although NaCl is the predominant salt in sea water it also contains divalent ions such as Ca^{2+} or Mg^{2+} which could lead to aggregate formation and flocculation of the sediment and thereby impacting C cycling (Grace et al., 1997).

4.2b Carbon – wet-dry vs flooding

In contrast to the salinity treatments, water level treatments had profound effects on C cycles under oligohaline conditions. Our experiments demonstrated no significant increase in CO_2 emission but significant decreases in CH_4 and DOC productions when comparing flooding to wet-dry treatments ($p < 0.05$) (Figs 3 a and b; c and d). Although re-flooding led to the highest CO_2 emission rate from soils at each wet-dry cycle, there was no significant difference in total CO_2–C emission between wet-dry and flooding treatments after 60-d incubations. Highest emissions of CO_2 were quantified immediately after rewetting. This results from an increase in C which most likely was caused by microbial biomass from cells death during the drying cycle as the decrease of soluble microbial byproduct-like from EEMs shown in Figs 6 a and b. Also, wet-dry treatments raised the exposure of organic residue**s** (Denef et al., 2001a, 2001b) due to the grinding of soil structure for exchange of wetting and drying process (Fierer and Schimel, 2002; Lundquist et al., 1999). These findings have been reported in laboratory and field experiment in peatland soil (Chow et al., 2006) and forest soils (Jarvis et al., 2007). However, the wet-dry treatment did not affect total CO_2-C loss in our study because of the offset of highest CO_2 emission rate at re-flooding and lowest CO_2 emission rate during the dry period. In sum, the wet-dry treatment resulted in 4.6-5.1% (CO_2-C /TC) C loss and flooding resulted in 4.4-4.9% C loss.

The drying cycle in the wet-dry treatments probably led to oxic conditions, and consequently might have inhibited the formation of CH_4 (Olsson et al., 2015). Only 0.1-0.2% of soil C was converted to CH_4–C in wet-dry treatments, and 1.0-1.2% in flooding treatments. Total C release from wet-dry treatments was 9.1-15.9% lower compared to flooding treatments. Our results are in line with previous results showing a decrease in CH_4 emissions in peatland soils and freshwater marsh when water table fluctuates (Moore and Knowles, 1989; Yang et al., 2013). Although wet-dry treatments did not affect total CO_2-C loss, there was a decrease in CH_4-C loss. Therefore, our data suggest that wet-dry treatments significantly decreased total C emissions (CO_2 + CH_4). These results are consistent with previous studies where fluctuating water tables reduced C emissions (Bass et al., 2014; Olsson et al., 2015).

Our study demonstrated that wet-dry treatments increased DOC production 1.1-1.6 fold after 60-d incubation. This was significantly lower compared to flooded treatments (1.7-1.9 fold) ($p < 0.05$). Researchers have shown that short heterotrophic microbial processes such as respiration and denitrification could lower DOC concentrations in wet-dry conditions more than that in flooding environments (Blodau and Moore, 2003; Burford and Bremner, 1975). Enhanced penetration of oxygen in wet-dry treatments resulted in an increase of both aerobic and anaerobic microbes (Fierer and Schimel, 2003; Lundquist et al., 1999). Also, the decrease in DOC concentration in wet-dry treatments could be attributed to altered microbial community structures during wet-drying process enhancing labile DOC consumption.

4.3 Nitrogen – salinity, water level (flooding and wet-dry)

In contrast to C biogeochemistry, significant changes were observed in N cycling in both saline and flooding treatments. An increase in salinity increased DN release but decreased N_2O emission from soils (Figs. 5 a, c). The increase in DN in water can be explained by ion exchange with NH_4^+ cations in soil with sodium cations (Na^+) in water (Wang and Sun, 2013). However, the increased availability of DN did not necessarily increase N_2O emission because high levels of salt can suppress both nitrification and denitrification (Osborne et al., 2015; Li et al., 2013). In addition to salinity, water level, which affects the availability of O_2 and redox status, could affect denitrification and N_2O production processes (Weitz et al., 2001; Lu et al., 2014). Continuous flooding limits the availability of oxygen in soils, reducing nitrification (Pezeshki and DeLaune, 2012). In contrast, wet–dry cycles allow O_2 penetration into the soil during dry periods, influencing microbial processes (i.e., substrate availability and microbial cell physiology) and soil physical properties, thus enhancing N_2O emissions (Stark and Firestone 1995; Burger et al., 2005; Kim et al., 2012) and increasing soil N losses (Borken and Matzner, 2009). Similar observations showing the effects of salt on N_2O and DN in wetlands have been reported previously (Azam and Ifzal, 2006; Chambers et al., 2013; Ardon et al., 2013).

4.4 Quality of DOM

SUVA is widely used as an indicator of aromatic C in soil and aquatic humic substances (Novak et al., 1992; Wang et al., 2015a; Yu et al., 2010). The E_2/E_3 ratio is inversely correlated with MW of DOM

(Hunt and Ohno, 2007; Wang et al., 2015b). In our study, not only did both, flooding and wet–dry cycle treatments increase DOC concentrations, they also increased the relative proportion of aromatic and humic-like compounds in soils (Fig.6), as indicated by a higher SUVA, FI and humic substance peak in region V in EEM and lower Freshness index (β/α) after 60-d incubation. In addition, a lower E_2/E_3 ratio in flooding treatments compared to wet-dry treatments after 60-d incubation suggests that DOM produced under flooding might mainly consist of compounds of higher molecular weight than that originating from wet-dry cycles. Such differences were attributed to the breakdown of large molecules by microorganisms under oxic conditions during the drying period (Chow et al., 2006; Krupa et al., 2012). Thus, increased MW, or recalcitrant DOM, limited microbial activities, resulting in the decrease of CO_2 and CH_4.

Conclusions and Outlook

Coastal wetland soils represent a large reservoir for global C, but the stability of this important C pool is endangered by rising sea level, which will cause seawater intrusion and alter the wetland hydroperiod. Our study demonstrated that low salt concentrations (<5 ppt) and changes in water contents can significantly affect GHG formation and DOM optical properties in coastal wetland soils, confirming that saltwater intrusion and water level fluctuation in coastal wetlands, due to sea level rise, can impact C and N cycles in this ecosystem. Noticeably, the impacts from fluctuating water level on C cycles are greater than from salt intrusion in oligohaline areas. In the low-lying coastal areas of the southeastern US, large inland freshwater forested wetlands have been experiencing changing water levels or hydroperiods due to rising water tables caused by sea level rise. The changes in C and N cycles in these wetlands could be significant and might lead to changes in the global budgets of climate-relevant greenhouse gases such as CH_4, CO_2, and N_2O. In combination with the presented kinetic model it might be possible to predict how formation of greenhouse gases (CO_2, CH_4) might be impacted by alterations in the carbon fractions in soil as a consequence of global climate change. However, in how far these results are also representative for other coastal wetlands or for processes in the environment is currently unknown. In addition, future studies and management efforts should also consider inland freshwater tidal wetlands, not just the salt-impacted areas, to evaluate how these environments might change as a consequence of sea level rise.

Acknowledgements

We gratefully acknowledge the Baruch Foundation for access to their land during the study. This research was partially supported by the NSF awards 1529927 and 1617040 and the U.S. Geological Survey, Climate and Land Use Change Research and Development Program, and was supported in part by the National Institute of Food and Agriculture, U.S. Department of Agriculture, under award numbers SC-1700489 and SC-1700424. Technical Contribution No. 6626 of the Clemson University Experiment Station. Dr. Liu was supported by the Chinese State Scholarship Fund from the China Scholarship Council (CSC).

References

Allen, J.A., Pezeshki, S.R., Chambers, J.L., 1996. Interaction of flooding and salinity stress on baldcypress (*Taxodium distichum*). Tree Physiology 16, 307–313. doi:10.1093/treephys/16.1-2.307

Ardón, M., Helton, A.M., Bernhardt, E.S., 2016. Drought and saltwater incursion synergistically reduce dissolved organic carbon export from coastal freshwater wetlands. Biogeochemistry 127, 411–426. doi:10.1007/s10533-016-0189-5

Ardón, M., Morse, J.L., Colman, B.P., Bernhardt, E.S., 2013. Drought-induced saltwater incursion leads to increased wetland nitrogen export. Glob. Chang. Biol. 19, 2976–2985. doi:10.1111/gcb.12287

Azam, F., Ifzal, M., 2006. Microbial populations immobilizing NH_4^+-N and NO_3^--N differ in their sensitivity to sodium chloride salinity in soil. Soil Biology and Biochemistry 38, 2491–2494. doi:10.1016/j.soilbio.2006.01.028

Bai, J., Gao, H., Xiao, R., Wang, J., Huang, C., 2012. A review of soil nitrogen mineralization as affected by water and salt in coastal wetlands: issues and methods. Clean - Soil, Air, Water 40, 1099–1105. doi:10.1002/clen.201200055

Baldwin, D.S., Rees, G.N., Mitchell, A.M., Watson, G., Williams, J., 2006. The short-term effects of salinization on anaerobic nutrient cycling and microbial community structure in sediment from a freshwater wetland. Wetlands 26, 455–464. doi:10.1672/0277-5212(2006)26[455:TSEOSO]2.0.CO;2

Bass, A.M., O'Grady, D., Leblanc, M., Tweed, S., Nelson, P.N., Bird, M.I., 2014. Carbon dioxide and methane emissions from a wet-dry tropical floodplain in northern Australia. Wetlands 34, 619–627. doi:10.1007/s13157-014-0522-5

546 Blodau, C., Moore, T.R., 2003. Micro-scale CO_2 and CH_4 dynamics in a peat soil during a water fluctuation
547 and sulfate pulse. Soil Biology and Biochemistry 35, 535–547.
548 doi:10.1016/S0038-0717(03)00008-7
549 Borken, W., Matzner, E., 2009. Reappraisal of drying and wetting effects on C and N mineralization and
550 fluxes in soils. Global Change Biology 15, 808–824. doi:10.1111/j.1365-2486.2008.01681.x
551 Bottner, P., 1985. Response of microbial biomass to alternate moist and dry conditions in a soil incubated
552 with ^{14}C- and ^{15}N-labelled plant material. . Soil Biology & Biochemistry 17, 329-337.
553 doi:10.1016/0038-0717(85)90070-7
554 Boyer, J.N., Groffman, P.M., 1996. Bioavailability of water extractable organic carbon fractions in forest
555 and agricultural soil profiles. Soil Biology & Biochemistry 28, 783–790.
556 doi:10.1016/0038-0717(96)00015-6
557 Breithaupt, J.L., Smoak, J.M., Smith, T.J., Sanders, C.J., Hoare, A., 2012. Organic carbon burial rates in
558 mangrove sediments: Strengthening the global budget. Global Biogeochemical Cycles 26,156–169.
559 doi:10.1029/2012GB004375
560 Burford, J.R., Bremner, J.M., 1975. Relationships between the denitrification capacities of soils and total,
561 water-soluble and readily decomposable soil organic matter. Soil Biology & Biochemistry 7, 389–
562 394. doi:10.1016/0038-0717(75)90055-3
563 Burger, M., Jackson, L.E., Lundquist, E.J., Louie, D.T., Miller, R.L., Rolston, D.E., Scow, K.M., 2005.
564 Microbial responses and nitrous oxide emissions during wetting and drying of organically and
565 conventionally managed soil under tomatoes. Biology and Fertility of Soils 42, 109–118.
566 doi:10.1007/s00374-005-0007-z
567 Busbee, W.S., Conner, W.H., Allen, D.M., Lanham, J.D., 2003. Composition and aboveground
568 productivity of three seasonally flooded depressional forested wetlands in coastal South Carolina.
569 Southeastern Naturalist 2, 335–346. doi:10.1656/1528-7092(2003)002[0335:CAAPOT]2.0.CO;2
570 Cayuela, M.L., Sánchez-Monedero, M.A., Roig, A., Sinicco, T., Mondini, C., 2012. Biochemical changes
571 and GHG emissions during composting of lignocellulosic residues with different N-rich by-products.
572 Chemosphere 88, 196–203. doi:10.1016/j.chemosphere.2012.03.001

573 Chambers, L.G., Davis, S.E., Troxler, T., Boyer, J.N., Downey-Wall, A., Scinto, L.J., 2014.
574 Biogeochemical effects of simulated sea level rise on carbon loss in an Everglades mangrove peat
575 soil. Hydrobiologia 726, 195–211. doi:10.1007/s10750-013-1764-6
576 Chambers, L.G., Osborne, T.Z., Reddy, K.R., 2013. Effect of salinity-altering pulsing events on soil
577 organic carbon loss along an intertidal wetland gradient: A laboratory experiment. Biogeochemistry
578 115, 363–383. doi:10.1007/s10533-013-9841-5
579 Chambers, L.G., Reddy, K.R., Osborne, T.Z., 2011. Short-Term Response of Carbon Cycling to Salinity
580 Pulses in a Freshwater Wetland. Soil Science Society of America Journal 75, 2000–2007.
581 doi:10.2136/sssaj2011.0026
582 Chow, A.T., Dahlgren, R.A., Zhang, Q., Wong, P.K., 2008. Relationships between specific ultraviolet
583 absorbance and trihalomethane precursors of different carbon sources. Journal of Water Supply:
584 Research and Technology - AQUA 57, 471–480. doi:10.2166/aqua.2008.064
585 Chow, A.T., Dai, J., Conner, W.H., Hitchcock, D.R., Wang, J.J., 2013. Dissolved organic matter and
586 nutrient dynamics of a coastal freshwater forested wetland in Winyah Bay, South Carolina.
587 Biogeochemistry 112, 571–587. doi:10.1007/s10533-012-9750-z
588 Chow, A.T., Tanji, K.K., Gao, S., 2003. Production of dissolved organic carbon (DOC) and trihalomethane
589 (THM) precursor from peat soils. Water Research 37, 4475–4485. doi:10.1016/S0043-
590 1354(03)00437-8
591 Chow, A.T., Tanji, K.K., Gao, S., Dahlgren, R.A., 2006. Temperature, water content and wet-dry cycle
592 effects on DOC production and carbon mineralization in agricultural peat soils. Soil Biology &
593 Biochemistry 38, 477–488. doi:10.1016/j.soilbio.2005.06.005
594 Cook, B.D., Allan, D.L., 1992. Dissolved organic carbon in old field soils - Compositional changes during
595 the biodegradation of soil organic matter. Soil Biology & Biochemistry 24, 595–600.
596 doi:10.1016/0038-0717(92)90085-C
597 Cormier, N., Krauss, K.W., Conner, W.H., 2013. Periodicity in stem growth and litterfall in tidal freshwater
598 forested wetlands: Influence of salinity and drought on nitrogen recycling. Estuaries and Coasts 36,
599 533–546. doi:10.1007/s12237-012-9505-z

600 Cory, R.M., McKnight, D.M., 2005. Fluorescence spectroscopy reveals ubiquitous presence of oxidized
601 and reduced quinones in dissolved organic matter. Environmental Science and Technology 39, 8142–
602 8149. doi:10.1021/es0506962
603 Davidson, E.A., Janssens, I.A., 2006. Temperature sensitivity of soil carbon decomposition and feedbacks
604 to climate change. Nature 440, 165–173. doi:10.1038/nature04514
605 Donato, D.C., Kauffman, J.B., Murdiyarso, D., Kurnianto, S., Stidham, M., Kanninen, M., 2011.
606 Mangroves among the most carbon-rich forests in the tropics. Nature Geoscience 4, 293–297.
607 doi:10.1038/ngeo1123
608 Fellman, J.B., Hood, E., Spencer, R.G.M., 2010. Fluorescence spectroscopy opens new windows into
609 dissolved organic matter dynamics in freshwater ecosystems: A review. Limnology and
610 Oceanography 55, 2452–2462. doi:10.4319/lo.2010.55.6.2452
611 Fierer, N., Allen, A.S., Schimel, J.P., Holden, P.A., 2003. Controls on microbial CO_2 production: A
612 comparison of surface and subsurface soil horizons. Global Change Biology 9, 1322–1332.
613 doi:10.1046/j.1365-2486.2003.00663.x
614 Fierer, N., Schimel, J.P., 2002. Effects of drying-rewetting frequency on soil carbon and nitrogen
615 transformations. Soil Biology and Biochemistry 34, 777–787. doi:10.1016/S0038-0717(02)00007-X
616 Goni, M.A., Gardner, L.R., 2003. Seasonal dynamics in dissolved organic carbon concentrations in a
617 coastal water-table aquifer at the forest-marsh interface. Aquatic Geochemistry 9, 209–232.
618 doi:10.1023/B:AQUA.0000022955.82700.ed
619 Gorban, A.N., Yablonsky, G.S., 2015. Three Waves of Chemical Dynamics, Mathematical Modelling of
620 Natural Phenomena 10, 1–5.
621 Grace, M.R., Hislop, T.M., Hart, B.T., Beckett, R., 1997. Effect of saline groundwater on the
622 aggregation and settling of suspended particles in a turbid Australian river. Colloids Surfaces
623 A Physicochem. Eng. Asp. 120, 123–141. doi:10.1016/S0927-7757(96)03863-0
624 Guha, H., Panday, S., 2012. Impact of sea level rise on groundwater salinity in a coastal community of
625 South Florida. Journal of the American Water Resources Association 48, 510–529.
626 Guldberg, C.M., Waage, P., 1864."Studies Concerning Affinity" C. M. Forhandlinger: Videnskabs-
627 Selskabet i Christiana, 35.

628 Hayashi, M., 2004. Temperature-electrical conductivity relation of water for environmental monitoring and
629 geophysical data inversion. Environmental Monitoring and Assessment 96, 119–128.
630 doi:10.1023/B:EMAS.0000031719.83065.68
631 Helms, J.R., Stubbins, A., Ritchie, J.D., Minor, E.C., Kieber, D.J., Mopper, K., 2008. Absorption spectral
632 slopes and slope ratios as indicators of molecular weight, source, and photobleaching of
633 chromophoric dissolved organic matter. Limonology and Oceanography 53, 955–969.
634 doi:10.4319/lo.2008.53.3.0955
635 Herbert, E.R., Boon, P., Burgin, A.J., Neubauer, S.C., Franklin, R.B., Ardón, M., Hopfensperger, K.N.,
636 Lamers, L.P.M., Gell, P., 2015. A global perspective on wetland salinization: ecological
637 consequences of a growing threat to freshwater wetlands. Ecosphere 6, art206.
638 doi:10.1890/ES14-00534.1
639 Hoff, J. H. van't (Jacobus Henricus van't), Cohen, E., Thomas, E. (1896-01-01), 1884. Studies in chemical
640 dynamics. Amsterdam: F. Muller; London: Williams & Norgate.
641 Hunt, J.F., Ohno, T., 2007. Characterization of fresh and decomposed dissolved organic matter using
642 excitation-emission matrix fluorescence spectroscopy and multiway analysis. Journal of Agricultural
643 and Food Chemistry 55, 2121–2128. doi:10.1021/jf063336m
644 IPCC, 2014. Climate Change 2014. Synthesis Report Summary Chapter for Policymakers. Ipcc.
645 Jarvis, P., Rey, A., Petsikos, C., Wingate, L., Rayment, M., Pereira, J., Banza, J., David, J., Miglietta, F.,
646 Borghetti, M., Manca, G., Valentini, R., 2007. Drying and wetting of Mediterranean soils stimulates
647 decomposition and carbon dioxide emission: the “Birch effect.” Tree Physiology 27, 929–940.
648 doi:10.1093/treephys/27.7.929
649 Kaiser, K., Guggenberger, G., Zech, W., 1996. Sorption of DOM and DOM fractions to forest soils.
650 Geoderma 74, 281–303. doi:10.1016/S0016-7061(96)00071-7
651 Kalbitz, K., Solinger, S., Park, J.-H., Michalzik, B., Matzner, E., 2000. Controls on the dynamics of
652 dissolved organic matter: A review. Soil Science 165, 277–304.
653 doi:10.1097/00010694-200004000-00001
654 Kim, D.-G., Vargas, R., Bond-Lamberty, B., Turetsky, M.R., 2012. Effects of soil rewetting and thawing
655 on soil gas fluxes: A review of current literature and suggestions for future research. Biogeosciences
656 9, 2459–2483. doi:10.5194/bg-9-2459-2012

657 Krauss, K.W., Whitbeck, J.L., 2012. Soil greenhouse gas fluxes during wetland forest retreat along the
658 lower Savannah River, Georgia (USA). Wetlands 32, 73–81. doi:10.1007/s13157-011-0246-8
659 Krupa, M., Spencer, R.G.M., Tate, K.W., Six, J., van Kessel, C., Linquist, B.A., 2012. Controls on
660 dissolved organic carbon composition and export from rice-dominated systems. Biogeochemistry
661 108, 447–466. doi:10.1007/s10533-011-9610-2
662 Lal, R., 2004. Soil carbon sequestration impacts on global climate change and food security. Science (80-
663 .). 304, 1623–1627 ST–Soil carbon sequestration impacts. doi:10.1126/science.1097396 [doi]\
664 Lewis, D.B., Brown, J.A., Jimenez, K.L., 2014. Effects of flooding and warming on soil organic matter
665 mineralization in Avicennia germinans mangrove forests and Juncus roemerianus salt marshes.
666 Estuarine, Coastal and Shelf Science 139, 11–19. doi:10.1016/j.ecss.2013.12.032
667 Liu, W.C., Liu, H.M., 2014. Assessing the impacts of sea level rise on salinity intrusion and transport time
668 scales in a tidal estuary, Taiwan. Water (Switzerland) 6, 324–344. doi:10.3390/w6020324
669 Lundquist, E.J., Jackson, L.E., Scow, K.M., 1999. Wet-dry cycles affect dissolved organic carbon in two
670 California agricultural soils. Soil Biology and Biochemistry 31, 1031–1038.
671 doi:10.1016/S0038-0717(99)00017-6
672 Marton, J.M., Herbert, E.R., Craft, C.B., 2012. Effects of salinity on denitrification and greenhouse gas
673 production from laboratory-incubated tidal forest soils. Wetlands 32, 347–357.
674 doi:10.1007/s13157-012-0270-3
675 Mitsch, W.J., Gosselink, J.G., 1993. Wetland. John Wiley & Sons, Inc. New York.
676 Montaño, N.M., García-Oliva, F., Jaramillo, V.J., 2007. Dissolved organic carbon affects soil microbial
677 activity and nitrogen dynamics in a Mexican tropical deciduous forest. Plant Soil 295, 265–277.
678 doi:10.1007/s11104-007-9281-x
679 Moore, T.R., Dalva, M., 2001. Some controls on the release of dissolved organic carbon by plant tissues
680 and soils. Soil Science 166, 38–47. doi:10.1097/00010694-200101000-00007
681 Moore, T.R., Knowles, R., 1989. The influence of water table levels on methane and carbon dioxide
682 emissions from peatland soils. Canadian Journal of Soil Science 69, 33–38. doi:10.4141/cjss89-004
683 Morillas, L., Durán, J., Rodríguez, A., Roales, J., Gallardo, A., Lovett, G.M., Groffman, P.M., 2015.
684 Nitrogen supply modulates the effect of changes in drying-rewetting frequency on soil C and N

685 cycling and greenhouse gas exchange. Global Change Biology 21, 3854–3863.
686 doi:10.1111/gcb.12956
687 Moseman-Valtierra, S., Gonzalez, R., Kroeger, K.D., Tang, J., Chao, W.C., Crusius, J., Bratton, J., Green,
688 A., Shelton, J., 2011. Short-term nitrogen additions can shift a coastal wetland from a sink to a source
689 of N_2O. Atmospheric Environment 45, 4390–4397. doi:10.1016/j.atmosenv.2011.05.046
690 Mosier, A.R., 1994. Nitrous oxide emissions from agricultural soils. Fertilizer Research 37, 191–200.
691 doi:10.1007/BF00748937
692 Moyano, F.E., Manzoni, S., Chenu, C., 2013. Responses of soil heterotrophic respiration to moisture
693 availability: An exploration of processes and models. Soil Biology & Biochemistry 59, 72–85.
694 doi:10.1016/j.soilbio.2013.01.002
695 Mulholland, P.J., 1981. Organic carbon flow in a swamp-stream ecosystem. Ecol. Monogr. 51,
696 307–322.doi:10.2307/2937276
697 Novak, J.M., Mills, G.L., Bertsch, P.M., 1992. Estimating the percent aromatic carbon in soil and aquatic
698 humic substances using ultraviolet absorbency spectrometry. Journal of Environmental Quality 21,
699 144–147.
700 Ohno, T., 2002. Fluorescence inner-filtering correction for determining the humification index of dissolved
701 organic matter. Environmental Science and Technology 36, 742–746. doi:10.1021/es0155276
702 Olsson, L., Ye, S., Yu, X., Wei, M., Krauss, K.W., Brix, H., 2015. Factors influencing CO_2 and CH_4
703 emissions from coastal wetlands in the Liaohe Delta, Northeast China. Biogeosciences 12, 4965–
704 4977. doi:10.5194/bg-12-4965-2015
705 Opio, A., Jones, M.B., Kansiime, F., Otiti, T., 2015. Dissolved organic carbon in a tropical wetland
706 dominated by *Cyperus papyrus*. Wetlands Ecology and Management 23, 1033–1038.
707 doi:10.1007/s11273-015-9437-z
708 Pathak, H., Rao, D.L.N., 1998. Carbon and nitrogen mineralization from added organic matter in saline
709 and alkali soils. Soil Biol. Biochem. 30, 695–702.
710 doi:http://dx.doi.org/10.1016/S0038-0717(97)00208-3
711 Pezeshki, S.R., DeLaune, R.D., 2012. Soil Oxidation-Reduction in wetlands and its impact on plant
712 functioning. Biology 1, 196–221. doi:10.3390/biology1020196
713 Rahmstorf, S., 2007. A semi empirical approach to projecting future sea-level rise. Science 315, 368–370.

714 doi:10.1126/science.1135456
715 Renaud, F.G., Le, T.T.H., Lindener, C., Guong, V.T., Sebesvari, Z., 2015. Resilience and shifts in agro-
716 ecosystems facing increasing sea-level rise and salinity intrusion in Ben Tre Province, Mekong Delta.
717 Climatic Change 133, 69–84. doi:10.1007/s10584-014-1113-4
718 Schofield, R. V., 2003. Application of salinization indicators and initial development of potential global
719 soil salinization scenario under climatic change. Global Biogeochem. Cycles 17, 1–13.
720 doi:10.1029/2002GB001935
721 Sholkovitz, E.R., 1976. Flocculation of dissolved organic and inorganic matter during the mixing of river
722 water and seawater. Geochim. Cosmochim. Acta 40, 831–845. doi:10.1016/0016-7037(76)90035-1
723 Setia, R., Gottschalk, P., Smith, P., Marschner, P., Baldock, J., Setia, D., Smith, J., 2013. Soil salinity
724 decreases global soil organic carbon stocks. The Science of the Total Environment 465, 267–72.
725 doi:10.1016/j.scitotenv.2012.08.028
726 Shi, A., Marschner, P., 2014. Changes in microbial biomass C, extractable C and available N during the
727 early stages of decomposition of residue mixtures. Soil Research 52, 366–372. doi:10.1071/SR13128
728 Silva, C.C., Guido, M.L., Ceballos, J.M., Marsch, R., Dendooven, L., 2008. Production of carbon dioxide
729 and nitrous oxide in alkaline saline soil of Texcoco at different water contents amended with urea: A
730 laboratory study. Soil Biology and Biochemistry 40, 1813–1822. doi:10.1016/j.soilbio.2008.03.004
731 Stuckey, B.N. 1982. Soil survey of Georgetown County South Carolina. Rep. Prepared for the Soil
732 Conservation Service, USDA, Washington, DC.
733 Wang, J.J., Dahlgren, R.A., Chow, A.T., 2015a. Controlled burning of forest detritus altering spectroscopic
734 characteristics and chlorine reactivity of dissolved organic matter: Effects of temperature and oxygen
735 availability. Environmental Science and Technology 49, 14019–14027. doi:10.1021/acs.est.5b03961
736 Wang, J.J., Dahlgren, R.A., Erşan, M.S., Karanfil, T., Chow, A.T., 2015b. Wildfire altering terrestrial
737 precursors of disinfection byproducts in forest detritus. Environmental Science and Technology 49,
738 5921–5929. doi:10.1021/es505836m
739 Wang, L., Sun, H., 2013. Prediction of Na^+ /NH_4^+ exchange in faujasite zeolite by molecular dynamics
740 simulation and thermodynamic integration method. The Journal of Physical Chemistry C 117, 14051–
741 14060. doi:10.1021/jp403326n

742 Wang, Y.L., Yang, C.M., Zou, L.M., Cui, H.Z., 2015. Spatial distribution and fluorescence properties of
743 soil dissolved organic carbon across a riparian buffer wetland in Chongming Island, China.
744 Pedosphere 25, 220–229. doi:10.1016/S1002-0160(15)60007-8
745 Weier, K.L., Doran, J.W., Power, J.F., Walters, D.T., 1993. Denitrification and the dinitrogen/nitrous oxide
746 ratio as affected by soil water, available carbon, and nitrate. Soil Science Society of America Journal
747 57, 66–72. doi:10.2136/sssaj1993.03615995005700010013x
748 Weitz, A.., Linder, E., Frolking, S., Crill, P.., Keller, M., 2001. N_2O emissions from humid tropical
749 agricultural soils: Effects of soil moisture, texture and nitrogen availability. Soil Biology &
750 Biochemistry 33, 1077–1093. doi:10.1016/S0038-0717(01)00013-X
751 Weston, N.B., Vile, M.A., Neubauer, S.C., Velinsky, D.J., 2011. Accelerated microbial organic matter
752 mineralization following salt-water intrusion into tidal freshwater marsh soils. Biogeochemistry 102,
753 135–151. doi:10.1007/s10533-010-9427-4
754 Woodruff, J.D., Irish, J.L., Camargo, S.J., 2013. Coastal flooding by tropical cyclones and sea-level rise.
755 Nature 504, 44–52. doi:10.1038/nature12855
756 Wu, C.Y., Liu, J.K., Cheng, S.H., Surampalli, D.E., Chen, C.W., Kao, C.M., 2010. Constructed wetland
757 for water quality improvement: A case study from Taiwan. Water Science and Technology 62, 2408–
758 2418. doi:10.2166/wst.2010.492
759 Xenopoulos, H.F.W.& M.A., 2009. Effects of agricultural land use on the composition of fluvial dissolved
760 organic matter. Nature Geoscience.
761 Yang, J., Liu, J., Hu, X., Li, X., Wang, Y., Li, H., 2013. Effect of water table level on CO_2, CH_4 and N_2O
762 emissions in a freshwater marsh of Northeast China. Soil Biology & Biochemistry 61, 52–60.
763 doi:10.1016/j.soilbio.2013.02.009
764 Yu, H., Xi, B., Su, J., Ma, W., Wei, Z., He, X., Guo, X., 2010. Spectroscopic properties of dissolved fulvic
765 acids: Anindicator for soil salinization in arid and semiarid regions in China. Soil Science 175, 240–
766 245. doi:10.1097/SS.0b013e3181e055b4
767 Zemke, K., Liebscher, A., Wandrey, M., 2010. Petrophysical analysis to investigate the effects of carbon
768 dioxide storage in a subsurface saline aquifer at Ketzin, Germany (CO_2SINK). International Journal
769 of Greenhouse Gas Control 4, 990–999. doi:10.1016/j.ijggc.2010.04.008

Zhu, B., Cheng, W., 2013. Impacts of drying-wetting cycles on rhizosphere respiration and soil organic matter decomposition. Soil Biology and Biochemistry 63, 89–96. doi:10.1016/j.soilbio.2013.03.027

Zsolnay, Á., 2003. Dissolved organic matter: Artefacts, definitions, and functions. Geoderma 113, 187–209. doi:10.1016/S0016-7061(02)00361-0

Figure Captions

Fig. 1 The relationship between (a) DOC-CO_2 and (b) DOC-CH_4 in surface forested wetland soil under permanent flooding.

Fig. 2 Formation rates of CO_2 (a-c), CH_4 (d-f), and N_2O (g-i) in surface forested wetland soil incubated at 0 ppt, 1 ppt, and 5 ppt sodium chloride under flooding with θ_g of 3.0 g-water g-soil^{-1} and wet-dry cycles with θ_g of 0.4~3.0 g-water g-soil^{-1}. The small diagram in the upper right hand corner of each figure is the cumulative emission over 60 days. Error bars represent the standard deviations of triplicate measurements. The vertical lines in each diagram indicate the 12-day wet-dry treatments. a-c variations are rate and total of CO_2-C emission among salinity, d-f variations are rate and total of CH_4-C emission among salinity; g-i are rate and total of N_2O-N emission among salinity during 60-d incubation

Fig.3 Variations in DOC (a-c), DN (d-f) and DOC/DN g-i) at 0, 1, and 5 ppt NaCl in surface forested wetland soil under flooding and wet-dry treatments during 60-d incubation. Error bar represents the standard deviation from triplicate measurements

Fig. 4 Variations in $SUVA_{254}$ (a-c). E_2/E_3 ratio (d-f) and S_R (g-i) in surface soils incubated at various salinities (0, 1, and 5 ppt NaCl) under flooding and wet-dry conditions over 60 days. Error bar represents the standard deviation from triplicate measurements

Fig. 5 A conceptual model for describing effect of water level and salinity on freshwater forested wetland soils. a and b are soil incubation with freshwater (0 ppt) experiencing flooding and wet-dry treatments, respectively; c and d are soil incubation with salt water (5 ppt) experiencing flooding and wet-dry treatments, respectively

Fig. 6 The quantity, quality and 3D fluorescence excitation emission matrices of DOC in forested wetland soil with salinity under flooding (A) and wet-dry (B) during 60-d incubation. The size of the pie chart represents the quantity of DOC, and the quality of DOC shows in each pie chart. A and B represent flooding and wet-dry treatment, respectively. Typical EEM figures are shown in Fig.6 C. Fluorescence regional integration can be used to quantify the fluorescent DOM by dividing EEM into five operationally defined regions: I) tyrosine-like; II) tryptophan-like; III) fulvic acid-like; IV) soluble microbial byproduct-like; and V), humic acid-like

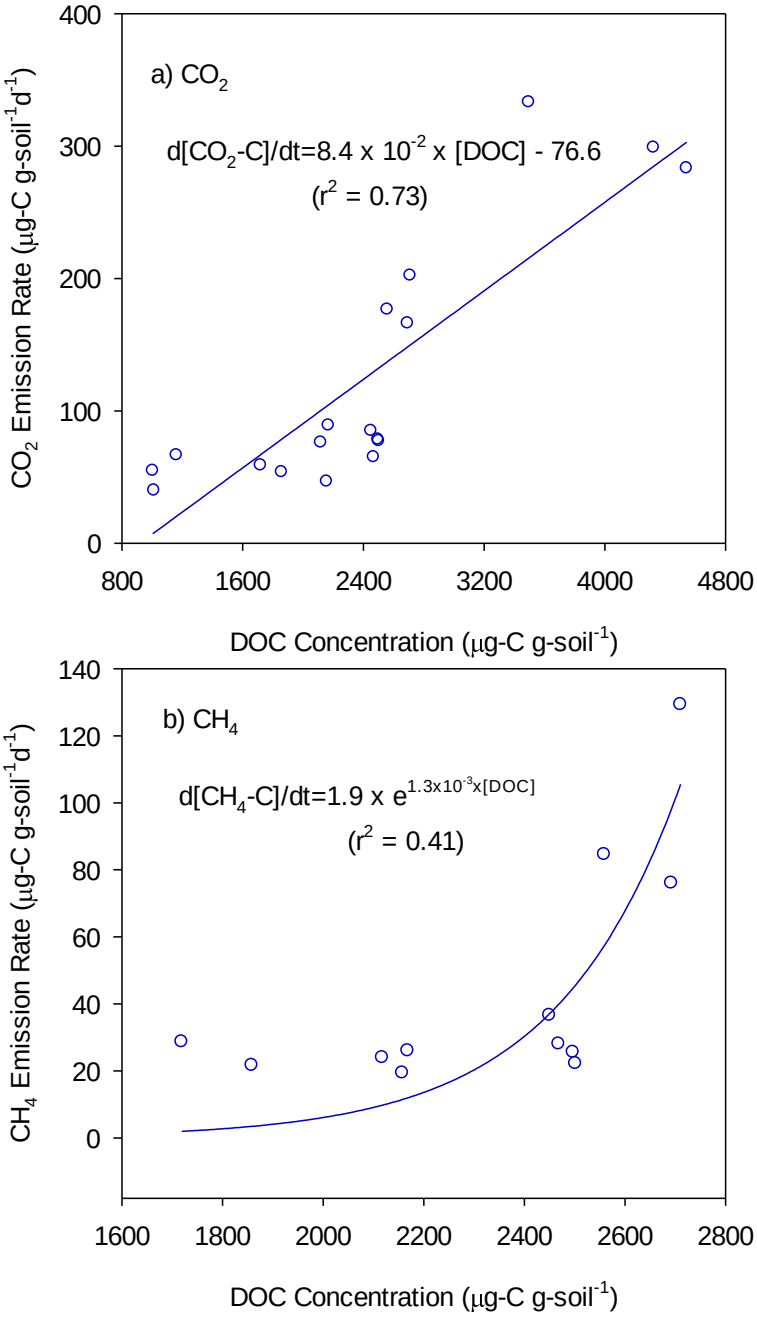

820

821

822 Fig. 1 The relationship between (a) DOC-CO_2 and (b) DOC-CH_4 in surface forested wetland soil under

823 permanent flooding.

824

825

826

827

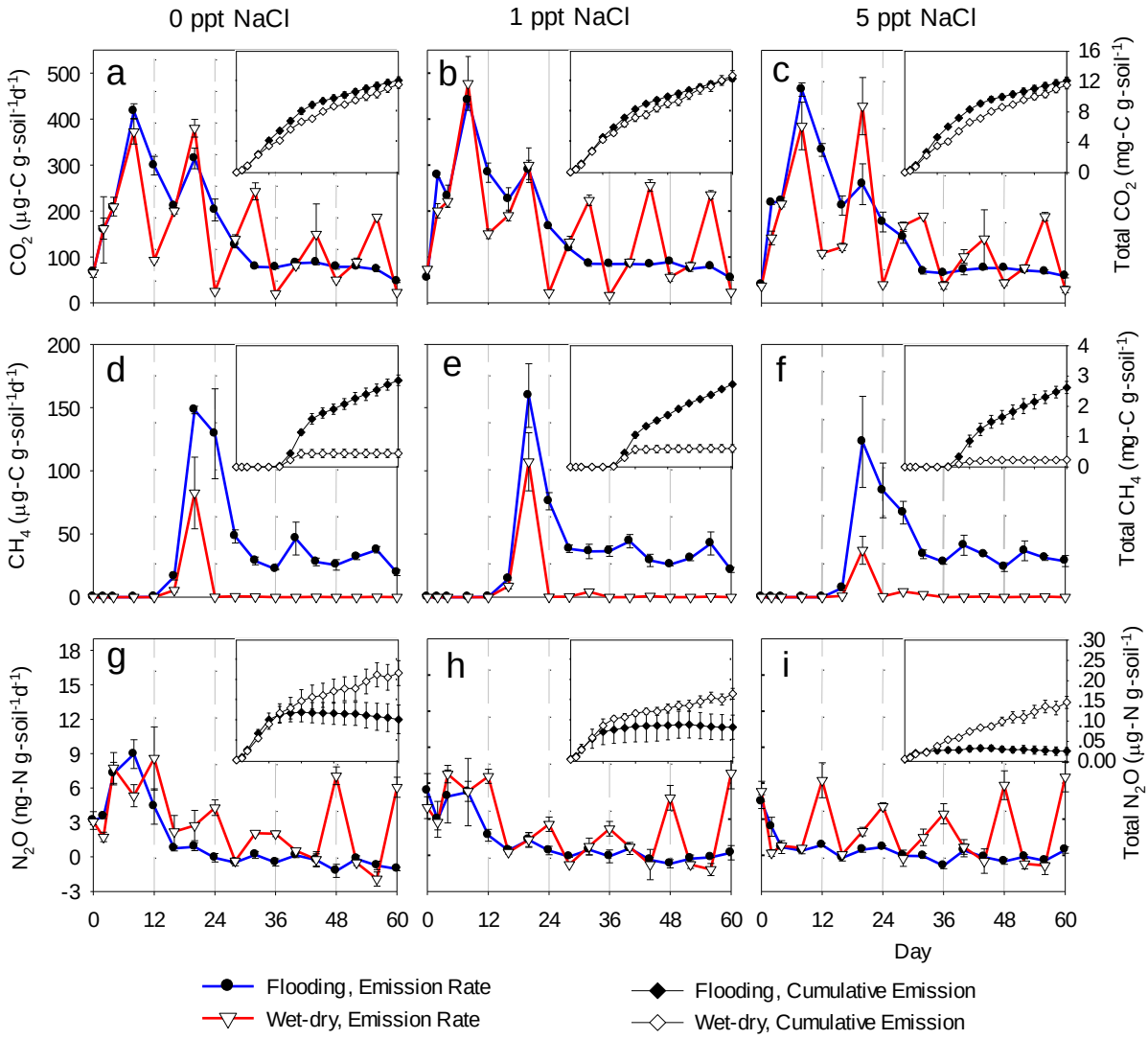

828

829 Fig. 2 Formation rates of CO_2 (a-c), CH_4 (d-f), and N_2O (g-i) in surface forested wetland soil incubated at
830 0 ppt, 1 ppt, and 5 ppt sodium chloride under flooding with θ_g of 3.0 g-water g-soil^{-1} and wet-dry cycles
831 with θ_g of 0.4~3.0 g-water g-soil^{-1}. The small diagram in the upper right hand corner of each figure is the
832 cumulative emission over 60 days. Error bars represent the standard deviations of triplicate measurements.
833 The vertical lines in each diagram indicate the 12-day wet-dry treatments. a-c variations are rate and total
834 of CO_2-C emission among salinity, d-f variations are rate and total of CH_4-C emission among salinity; g-i
835 are rate and total of N_2O-N emission among salinity during 60-d incubation

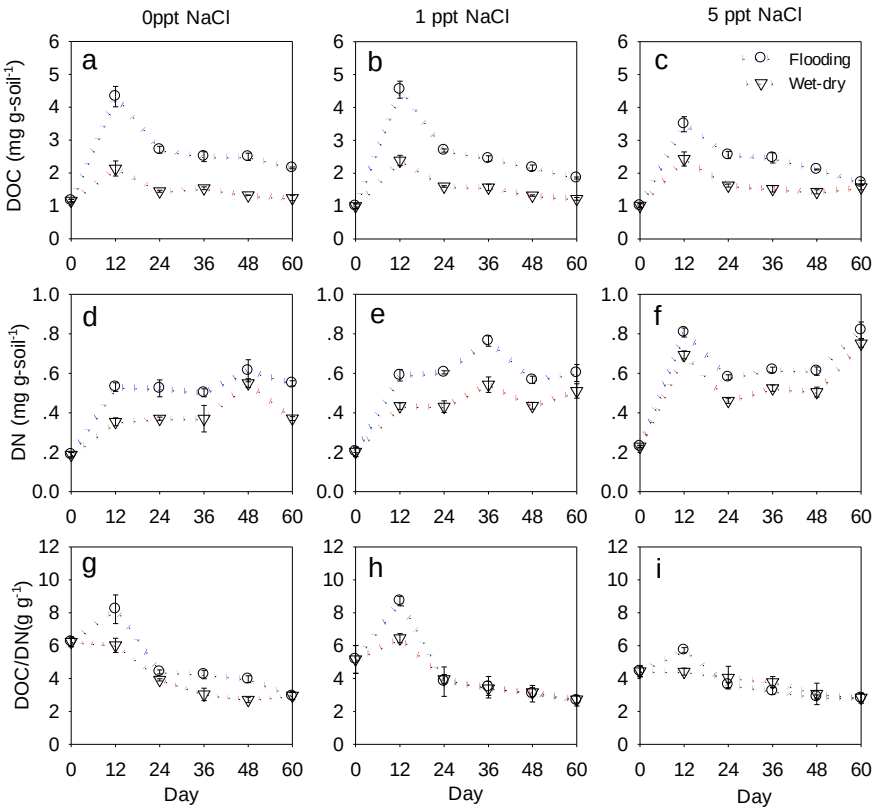

Fig.3 Variations in DOC (a-c), DN (d-f) and DOC/DN g-i) at 0, 1, and 5 ppt NaCl in surface forested wetland soil under flooding and wet-dry treatments during 60-d incubation. Error bar represents the standard deviation from triplicate measurements

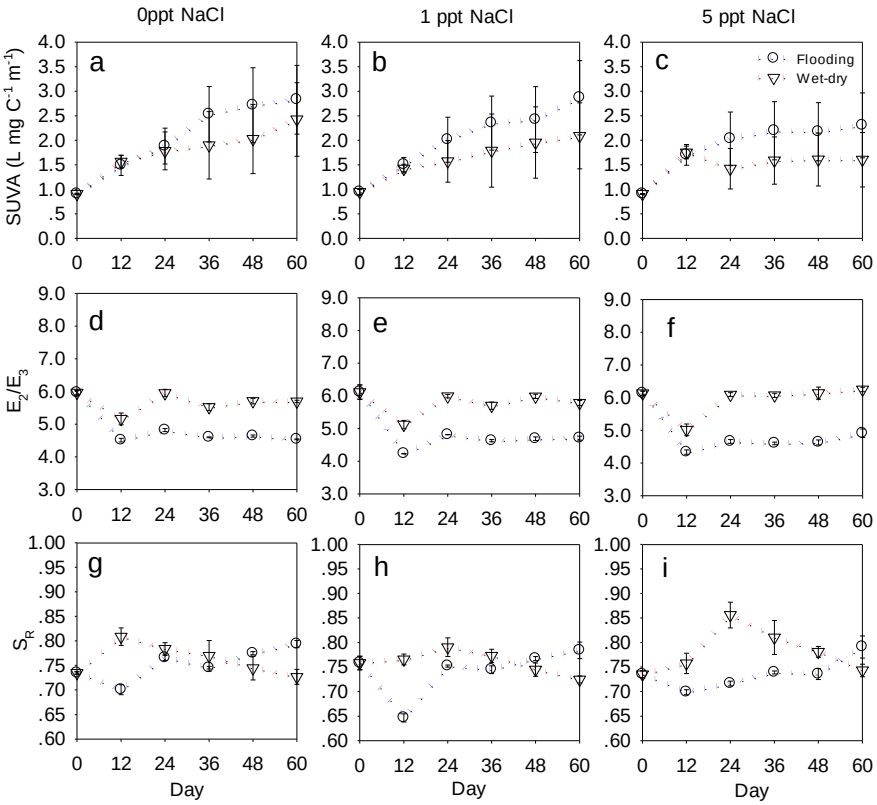

Fig. 4 Variations in $SUVA_{254}$ (a-c). E_2/E_3 ratio (d-f) and S_R (g-i) in surface soils incubated at various salinities (0, 1, and 5 ppt NaCl) under flooding and wet-dry conditions over 60 days. Error bar represents the standard deviation from triplicate measurements

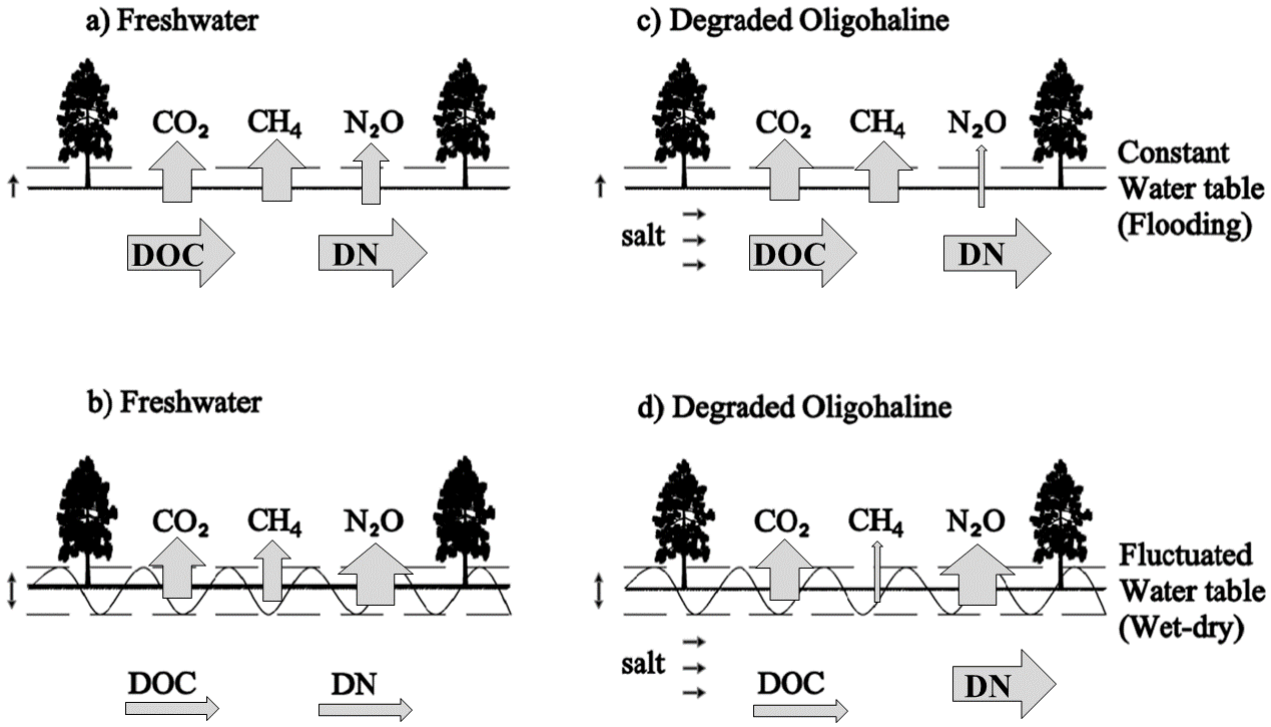

Fig. 5 A conceptual model for describing effect of water level and salinity on freshwater forested wetlands. a and b are soil incubation with freshwater (0 ppt) experiencing flooding and wet-dry treatments, respectively; c and d are soil incubation with degraded oligohaline (5 ppt) experiencing flooding and wet-dry treatments, respectively.

882

883

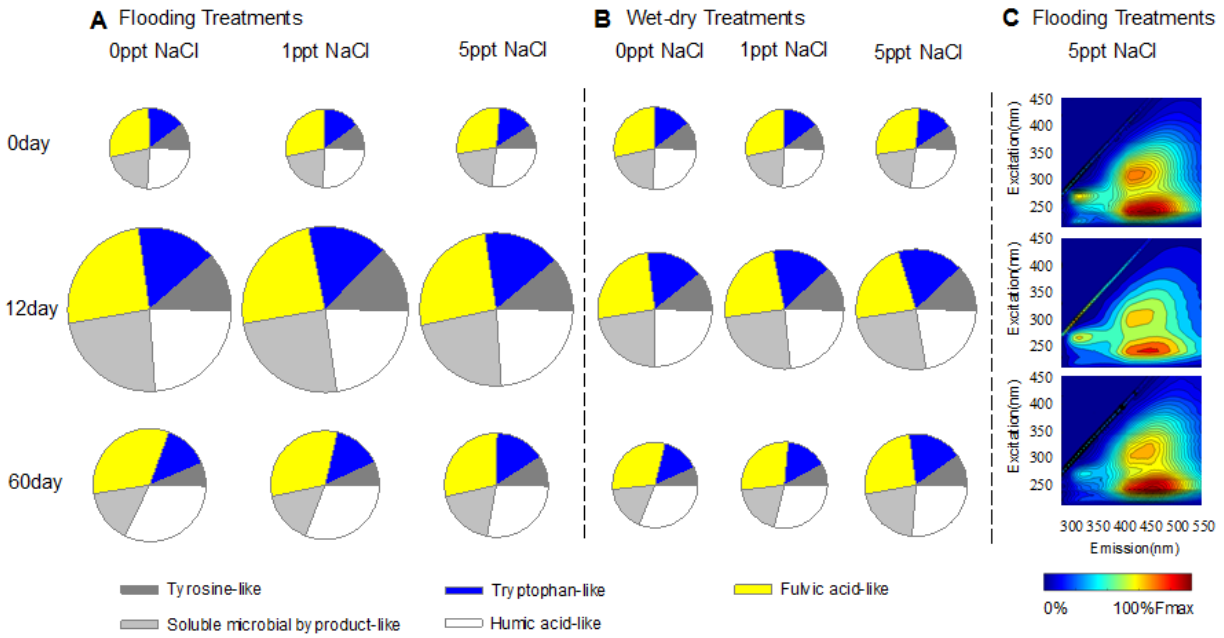

884

885 Fig. 6 The quantity, quality and 3D fluorescence excitation emission matrices of DOM in forested wetland
886 soil with salinity under flooding (A) and wet-dry (B) during 60-d incubation. The size of the pie chart
887 represents the quantity of DOM, and the quality of DOM shows in each pie chart. A and B represent
888 flooding and wet-dry treatment, respectively. Typical EEM figures are shown in Fig.6 C. Fluorescence
889 regional integration can be used to quantify the fluorescent DOM by dividing EEM into five operationally
890 defined regions: I) tyrosine-like; II) tryptophan-like; III) fulvic acid-like; IV) soluble microbial byproduct-
891 like; and V), humic acid-like.

892

893

894

895

896

897

898

Tables

Table 1. Soil properties of surface forested wetland soils (mean ± standard deviation, n=3)

Parameters	Original soil
pH	5.0±0.1
Electrical conductivity (EC_{25}) (mS cm^{-1})	7.6±3.1
Dissolved organic carbon (mg g-$soil^{-1}$)	1.2±0.0
Total dissolved nitrogen (mg g-$soil^{-1}$)	0.2±0.0
Total carbon (TC) (mg g-$soil^{-1}$)	240.9±4.0
Total nitrogen (TN) (mg g-$soil^{-1}$)	17.3±1.0
C:N ratio	13.9±0.3

Table 2. Total emissions of carbon dioxide, methane and nitrous oxide with salinity and soil water content during 60-d incubation. (mean ± standard deviation, n=3)

Water level	Salinity	CO_2-C loss (mg-C g-$soil^{-1}$)	CH_4 -C loss (mg-C g-$soil^{-1}$)	Total loss (CO_2-C + CH_4-C) (mg-C g-$soil^{-1}$)	N_2O-N loss (μg-N g-$soil^{-1}$)
flooding	0ppt	12.2 ± 0.5 [a]	2.9±0.2 [a]	15.1±0.4 [a]	0.10±0.04[ad]
	1ppt	12.4±0.4 [a]	2.7±0.1 [a]	15.2±0.3 [a]	0.08±0.03[ab]
	5ppt	12.2±0.5 [a]	2.6±0.2 [a]	14.8±0.7 [a]	0.02±0.01[b]
wet-dry	0ppt	11.7±0.5 [a]	0.5±0.1 [b]	12.1±0.6 [b]	0.22±0.03[c]
	1ppt	12.8±0.7 [a]	0.6±0.1 [b]	13.4±0.5 [b]	0.17±0.01[cd]
	5ppt	11.6±0.5 [a]	0.2±0.1 [b]	11.8±0.5[b]	0.15±0.02[ac]

Different letters represent significantly different means ($p<0.05$) based on one-way ANOVA.

Supplementary Information

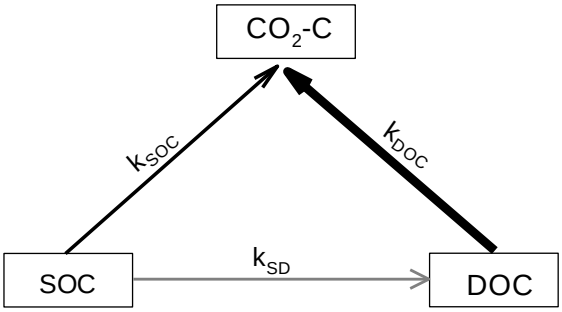

Box

CO_2-C:

[1] $d[CO_2\text{-}C]/dt=k_{SOC}[SOC]+k_{DOC}[DOC]$

[2] $d[CO_2\text{-}C]/dt=k_{SOC}([TAOC]-[DOC])+k_{DOC}[DOC]$

[3] $d[CO_2\text{-}C]/dt=(k_{DOC}-k_{SOC})[DOC])+k_{SOC}[TAOC]$

[4] $d[CO_2\text{-}C]/dt=k_{app}[DOC]+k_{SOC}[TAOC]$

SOC: Soil organic carbon ($\mu g\text{-}C\ g\text{-}soil^{-1}$)

DOC: Dissolved organic carbon ($\mu g\text{-}C\ g\text{-}soil^{-1}$)

TAOC: Total available organic carbon ($\mu g\text{-}C\ g\text{-}soil^{-1}$)

TAOC = SOC + DOC

k_{SOC}: reaction rate constant for C mineralization (d^{-1}) utilizing SOC to produce CO_2-C

k_{DOC}: reaction rate constant for C mineralization (d^{-1}) utilizing DOC to produce CO_2-C

k_{SD}: reaction rate constant for C mineralization (d^{-1}) utilizing SOC to produce DOC

k_{app}: apparent rate constant for overall C transfer to CO_2-C (d^{-1})

Fig.s1 A conceptual model describing CO_2 and CH_4 production in freshwater forested wetland soils

931 **Table s1 Salinity and soil water content used in the incubation experiments**

Soil used	Treatment	Incubation conditions	
		Variables	Constant parameters
Surface soil	Salinity effect	S=0, 1, 5	θ_g=3.0
	Wet-dry cycles	θ_g=0.4-3.0	S=0,1, 5

932 *θ_g is soil water content in g-water g-soil^{-1} and S is salinity in ppt (1 part in one trillion parts of water*
933 *solution).*

934

935

936

937

938 **Table s2. The pH and EC (mean ± standard deviation; n=3) of forested wetland soil during 60-d**
939 **incubation**

Parameters	water level	salinity (NaCl)	incubation(day)					
			0	12	24	36	48	60
pH	flooding	0ppt	5.0±0.1^{a}	6.4±0.4^{ad}	7.9±0.2^{a}	7.4±0.1^{a}	7.3±0.1^{a}	7.5±0.0^{a}
		1ppt	4.8±0.1^{a}	5.9±0.1^{ac}	7.6±0.0^{a}	7.2±0.0^{a}	7.3±0.0^{a}	7.2±0.6^{a}
		5ppt	4.8±0.1^{a}	6.2±0.3^{adc}	6.6±0.2^{b}	6.2±0.2^{b}	5.7±0.1^{b}	6.2±0.4^{b}
	wet-dry	0ppt	5.0±0.1^{a}	6.3±0.2^{adc}	6.5±0.3^{b}	6.2±0.1^{b}	5.9±0.0^{b}	6.1±0.1^{b}
		1ppt	4.8±0.1^{a}	6.3±0.2^{ad}	6.7±0.1^{b}	6.2±0.3^{b}	5.2±0.7^{b}	5.9±0.1^{b}
		5ppt	4.8±0.1^{a}	5.7±0.1^{c}	6.4±0.2^{b}	6.1±0.1^{b}	5.5±0.2^{b}	5.9±0.1^{b}
$EC_{25℃}$ (mS/cm)	flooding	0ppt	4.6±3.1^{a}	4.1±0.1^{ac}	4.0±0.4^{a}	3.5±1.0^{a}	3.6±0.3^{a}	3.9±0.0^{a}
		1ppt	6.4±3.1^{a}	5.6±0.2^{a}	5.1±0.0^{a}	4.8±0.1^{ac}	5.7±0.0^{ac}	6.0±0.1^{a}
		5ppt	13.5±0.1^{b}	11.5±0.2^{b}	11.4±0.4^{b}	12.7±0.1^{b}	14.0±0.0^{b}	14.1±0.1^{b}
	wet-dry	0ppt	4.6±0.3^{a}	2.9±0.6^{c}	3.1±0.4^{a}	3.4±0.2^{a}	3.8±0.1^{ac}	4.0±0.1^{a}
		1ppt	6.4±0.3^{a}	4.2±0.7^{ac}	4.3±0.7^{a}	5.2±2.4^{ac}	6.0±0.0^{c}	6.1±0.1^{a}
		5ppt	13.5±0.1^{b}	10.7±0.7^{b}	10.5±0.7^{b}	9.1±2.4^{d}	13.4±0.4^{b}	13.8±0.1^{b}

940 *Different letters represent significantly different means ($p<0.05$) based on a one-way ANOVA.*

941

942 **Table s3 Fluorescence Index and Freshness Index of DOC during 60-d incubation**

Parameters	Water level	Salinity	Incubation(day)					
			0	12	24	36	48	60
Fluorescence Index	Flooding	0ppt	1.51	1.44	1.46	1.45	1.44	1.46
		1pp	1.50	1.47	1.45	1.46	1.47	1.45
		5ppt	1.55	1.45	1.49	1.47	1.51	1.51
	Wet-dry	0ppt	1.51	1.47	1.47	1.51	1.47	1.47
		1ppt	1.50	1.47	1.49	1.5	1.49	1.48
		5ppt	1.55	1.52	1.52	1.5	1.53	1.48
Freshness Index	Flooding	0ppt	0.56	0.55	0.52	0.51	0.52	0.50
		1pp	0.57	0.56	0.53	0.53	0.52	0.53
		5ppt	0.58	0.58	0.57	0.56	0.57	0.57
	Wet-dry	0ppt	0.56	0.56	0.6	0.61	0.63	0.63
		1ppt	0.57	0.56	0.61	0.61	0.63	0.65
		5ppt	0.58	0.60	0.66	0.64	0.64	0.66

943